Delft University of Technology

A Rigorous Analysis of the Random Noise in Reflection Coefficients Synthesized via Mixed-Signal Active Tuners

Mubarak, Faisal ; Muñoz, Fabio; Spirito, Marco

Citation (APA)
Mubarak, F., Muñoz, F., & Spirito, M. (2023). A Rigorous Analysis of the Random Noise in Reflection Coefficients Synthesized via Mixed-Signal Active Tuners. In *Proceedings of the 2023 101st ARFTG Microwave Measurement Conference (ARFTG): Challenges in Complex Measurement Environments, ARFTG 2023* (pp. 1-4). (101st ARFTG Microwave Measurement Conference: Challenges in Complex Measurement Environments, ARFTG 2023). IEEE. https://doi.org/10.1109/ARFTG57476.2023.10279048

Important note
To cite this publication, please use the final published version (if applicable).
Please check the document version above.

A Rigorous Analysis of the Random Noise in Reflection Coefficients Synthesized via Mixed-Signal Active Tuners

Faisal Mubarak[1,2], Fabio Munoz[1], Marco Spirito[2]
[1]Van Swinden Laboratorium (VSL), Delft, The Netherlands
[2]Electronics Circuits and Architechtures Group (ELCA), Delft University of Technology, The Netherlands
[1]fmubarak@vsl.nl

Abstract — In this contribution, we present a rigorous analysis based on uncertainty propagation techniques to estimate the random variation of the controlled reflection coefficient in mixed-signal load-pull test benches. A digital-to-analog converter is commonly used in these test benches to generate the baseband signal required to synthesize the high-frequency, user-defined injected wave. To study the random noise of the injected wave, which can be mapped to the noise of the controlled reflection coefficient, we employ Jacobian sensitivity functions between the baseband signal and the RF one. First, the baseband integrated rms noise of the up-converter is evaluated, and then the upconverted noise is determined via the derived transfer function. Finally, experimental results to validate the uncertainty control bound of the synthesized reflection coefficients are presented, highlighting a full coverage of the measured reflection coefficients.

Keywords — S-parameter noise, frequency domain noise, residual-error, noise analysis, uncertainty analysis, vector network analyzer (VNA).

I. INTRODUCTION

From their introduction [1], load-pull techniques have provided an experimental means to validate devices and circuit performances in different impedance ranges. These techniques have quickly become an indispensable (experimental) tool to validate the device model and identify optimal loading conditions for the user-selected performance metrics. Throughout the years, load-pull test benches have been developed using passive, active closed-loop and open-loop topologies [2]. After its introduction to enable the wideband modulated signal harmonic load-pull [3], the mixed-signal open-loop topology has become the leading architecture, enabling high-speed [4] non-linear device characterisation up to (sub)mm-wave bands [5]. Mixed-signal architectures employ, in their most simple implementation, a high-resolution digital-to-analog converter (DAC) signal, which is upconverted and vector modulated, employing an IQ mixing stage, to the carrier frequency driving the device under test (DUT). The mixing function upconverts the baseband noise generated by the DAC cards, mixing it with the phase noise of the carrier frequency synthesiser. This mixing process and the instruments used in the test bench then define the noise of the vector-modulated wave, which synthesises the user-desired reflection coefficients. Due to their architecture and the non-linear nature of the DUT, open-loop topologies require the usage of convergence algorithms to reach the desired reflection coefficient. For this reason, the noise of the vector-modulated wave (intrinsically) defines the convergence resolution limit in practical measurement, i.e., when measurement time needs to be optimised. While previous contributions have analysed the uncertainties of large-signal metrics in 50 Ohm [6] and non-50 Ohm (i.e., load pull) environments [7], this contribution focuses on quantifying and providing an error bound for the random noise in the reflection coefficients synthesised via mixed-signal active tuners. This noise contribution is an important parameter when attempting to optimise the (rms noise) of the up-conversion elements composing the active tuners to minimise the convergence algorithm errors and when implementing the complete uncertainty propagation framework of active load pull test benches [8], [9], [10], [11]. The paper is organised as follows, first, the considered tuner architecture is described and analysed for its transfer function (i.e., baseband to carrier frequency). Then, the tuner model is employed to determine the Jacobian matrix, which propagates the DAC noise contribution to the amplitude and phase error of the synthesised injected wave. Finally, the proposed approach is validated by comparing measurements and calculated reflection coefficient noise for varying load impedances set by the active tuner sensitivity coefficients.

II. MEASUREMENT UNCERTAINTY

This section details the noise sources involved in vector network analyser (VNA) measurements which can be grouped into two main categories, i.e., additive noise (σ_a) and multiplicative noise (σ_m) sources. While [8] identifies VNA measurement noise contribution as marginal, it is a critical factor in measurements demanding high-resolution performance [12]. A measurement noise model identifying σ_a and σ_m noise sources in a VNA by [12] is shown in the following:

$$\sigma|\Gamma_T| = \sigma_a + \sigma_m \cdot |\Gamma_T| \tag{1}$$

$$\sigma\angle\Gamma_T = tan^{-1}\left(\frac{\sigma_a}{|\Gamma_T|}\right) \tag{2}$$

Here, $\sigma|\Gamma_T|$ is the noise on the magnitude, and $\sigma\angle\Gamma_T$ represents the noise on the phase components of the measured reflection coefficient Γ_T. We employ this method to analyse the noise of the reflection coefficient when a passive termination is employed or when the same termination is

synthesised by the active tuner described in section IV. Figure 1 shows measurement noise results for active and passive tuners, depicted with markers. The tuner synthesised a reflection coefficient magnitude ($|\Gamma_T|$) of 0.6 to the VNA, and the operational frequency was set at 6 GHz. The bounded area indicated with a red line represents the calculated noise of the reflection coefficient when only the VNA receiver noise is considered. The noise contribution is severely underestimated in the measurement systems employing active tuners.
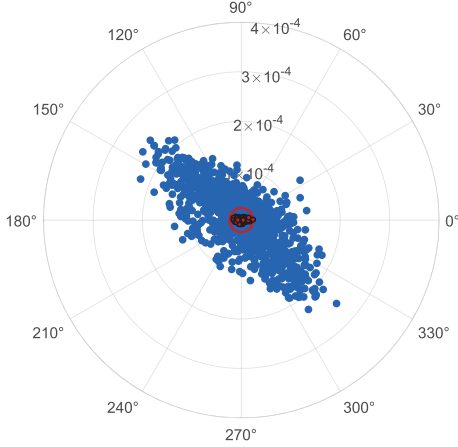

Fig. 1. Reflection coefficient measurement noise for active (blue markers) and passive (red markers) tuners with $|\Gamma_T| \approx 0.6$ at 6 GHz. The bounded area indicated with the red line represents the calculated noise contribution.

It is clear that the noise behaviour of a VNA is substantially affected by the mixed signal tuner and needs a rigorous analysis for accurate noise evaluation. In section III, a method is proposed to accurately determine σ_a for active tuners using DAC noise results and subsequently estimate $\sigma|\Gamma_T|$, and $\sigma\angle\Gamma_T$ using (1) and (2). For estimating σ_m, method outlined in [8] is used.

III. MIXED-SIGNAL TUNER TRANSFER FUNCTION

This section details the method proposed for developing the active tuner transfer function, suitable for the propagation of IQ-baseband noise uncertainties to RF Γ_T uncertainties. Figure 2 depicts the simplified block scheme of the mixed signal tuner used for this work.

First, the Copper Mountain VNA (C2420) is calibrated using a short-open-load (SOL) calibration method using traceable 3.5 mm coaxial standards at VSL. The measurement system is calibrated at several frequencies ranging from 2 GHz up to 18 GHz with 4 GHz steps, as this is also the operational range of the active tuner. Subsequently, the calibrated tuner reflection coefficient Γ_T is measured for a range of v_I and v_Q DC voltage values. These voltages represent the baseband In-phase (v_I) and Quadrature-phase (v_Q) signals applied to the upconverter. The voltages are generated with a multi-channel 24-bit DAC from the Nation Instruments NI-9260 platform. The magnitude of the IQ vector ($|IQ|$) ranges from 10-4 up to 0.08 V, with a logarithmic distribution. We sweep the IQ phase ($\angle IQ$) from 0 to 360 degrees at each IQ-magnitude value with
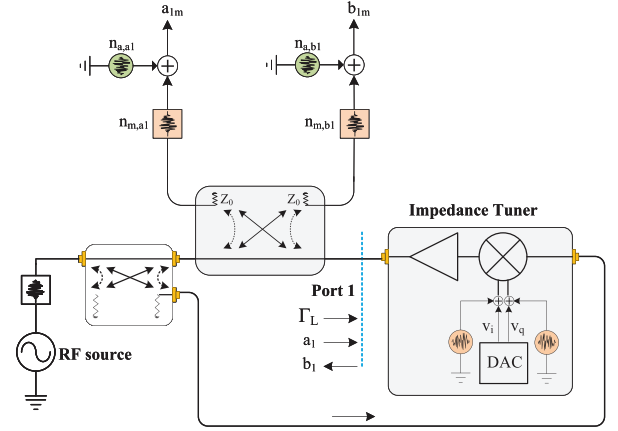

Fig. 2. Overview of the measurement set-up used for the development of the impedance tuner behavioural model. The depicted active tuner uses IQ-mixer for controlling the tuner reflection coefficient with DC in- and quadrature-phase voltages.

a 45-degree step size. The 45-degree step size is acceptable as Γ_T sensitivity for IQ magnitude is critical. The results of this experiment are shown with red markers in Fig. 3.

Polynomial fits are determined to model identical behaviour corresponding to the measurement results with closed-form equations. These closed-form equations allow calculating the sensitivity coefficients between the IQ-baseband voltages and Γ_T needed for uncertainty propagation. The acquired polynomial fits of the data are described as follows:

$$|\Gamma_T(|IQ|, \angle IQ)| = a_0 + \sum_{n=1}^{5}\left(|IQ|^n \sum_{m=1}^{2} \angle IQ^m \cdot b_m\right) \quad (3)$$

$$\angle\Gamma_T(|IQ|, \angle IQ) = c_0 + \sum_{n=1}^{5}\left(|IQ|^n \sum_{m=1}^{2} \angle IQ^m \cdot d_m\right) \quad (4)$$

For brevity, only results of the magnitude polynomial equation are shown in Fig. 3. The modulus and phase of the
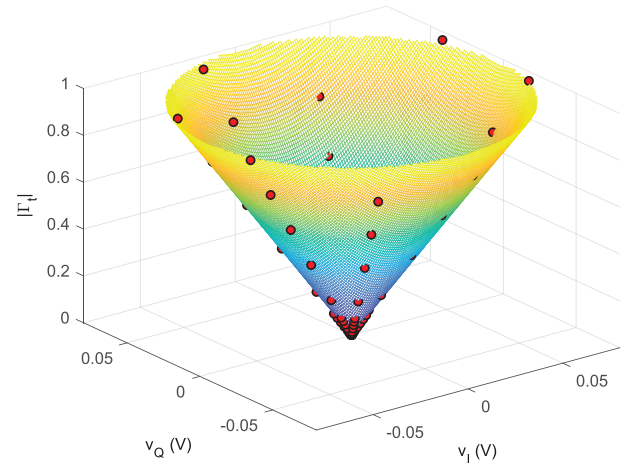

Fig. 3. The IQ-mixer transfer function results for magnitude component at 4 GHz.

reflection coefficient dependency on the baseband IQ vector are incorporated in the Jacobian matrix shown below.

$$J_T = \begin{bmatrix} \frac{\partial |\Gamma_T|}{\partial |IQ|} & \frac{\partial |\Gamma_T|}{\partial \angle IQ} \\ \frac{\partial \angle \Gamma_T}{\partial |IQ|} & \frac{\partial \angle \Gamma_T}{\partial \angle IQ} \end{bmatrix} \quad (5)$$

Finally, using the covariance matrix containing the IQ-baseband noise values shown in (6) and the Jacobian matrix, determined in (5), we can calculate tuner reflection coefficient noise using (7). We assume no correlation between both components in the covariance matrix, so off-diagonal values are set to zero in (6) and (7).

$$\Sigma_{IQ} = \begin{bmatrix} \sigma^2_{|IQ|} & \\ & \sigma^2_{\angle IQ} \end{bmatrix} \quad (6)$$

$$\Sigma_T = \begin{bmatrix} \sigma^2_{a,m} & \\ & \sigma^2_{a,p} \end{bmatrix} = J_T \cdot \Sigma_{IQ} \cdot J_T^T \quad (7)$$

Here, $\sigma^2_{a,m}$ and $\sigma^2_{a,p}$ are the additive noise in the magnitude and phase components. As it concerns an additive noise source, the phase of the noise vector is considered to be within 0 and 360 degrees with an equal probability. Hence, the effect of $\sigma^2_{a,p}$ is negligible as $\sigma^2_{a,m}$ will set the noise-floor.

IV. MEASUREMENT EXPERIMENT AND DISCUSSION

In this section, first, we describe the measurements of the noise values corresponding to the v_I and v_Q DC voltages generated by the DAC. Subsequently, the DC noise values $\sigma^2_{|IQ|}$ and $\sigma^2_{\angle IQ}$ corresponding to v_I and v_Q are propagated using the proposed method for calculating the corresponding Γ_T reflection coefficient noise. Finally, the approach is validated by comparing the calculated and measured noise values at various active tuner Γ_T values.
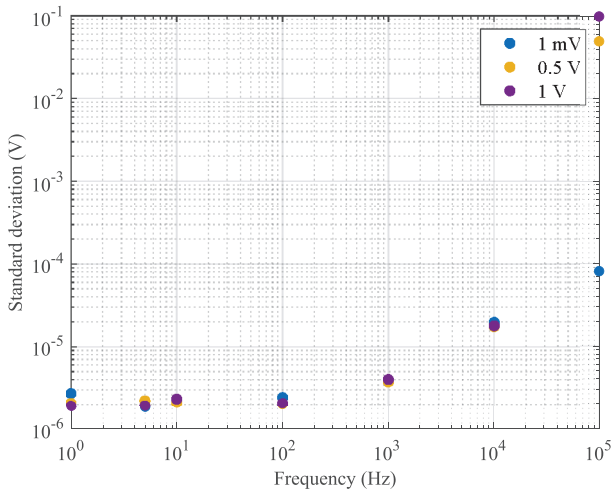

Fig. 4. DC source noise measurement results for I and Q channel DC voltages as function of equivalent integration frequency.

A. DC Noise measurement

A multi-channel NI-9260 DAC provides the DC voltages v_I and v_Q needed to control the tuner Γ_T. The DAC has two voltage output channels with a 24-bit analogue output resolution and a sampling rate of 51.2 kS/s. The DC noise level of the I-channel (σ^2_I) and Q-channel (σ^2_Q) is measured to determine the noise contribution of the DAC. For that, DC voltages v_I and v_Q were generated and measured using an HP-3458A multimeter. Different integration times were set in the multimeter, and 1000 samples were collected for each voltage and integration time. Because the integration time acts as a low-pass filter for the noise, the equivalent cutoff frequency is calculated by taking the inverse of the integration time. The noise is calculated by taking the standard deviation of the samples recorded. Fig. 4 depicts the noise results for ($\sigma^2_{|I|}$) and ($\sigma^2_{|Q|}$) as the standard deviation versus the equivalent integration frequency. The noise is measured for three different v_I and v_Q values covering the range of Γ_T values that the active tuner will generate. The noise remains similar for the three voltage levels tested; above the 10 kHz, it shows a dependency on the voltage level set at the DC source.

B. Tuner Noise Measurements

First, we use active and passive tuners to characterise the reflection coefficient measurement noise. The tuner described in Fig. 2 is used. The VNA test-port power level is set at -10 dBm, and Intermediate Frequency Bandwidth (IFBW) is set at 7 Hz. Subsequently, the tuner is connected to the VNA and set to generate reflection coefficients ranging from 0 to 1 using v_I and v_Q signals provided by the NI DAC. At each tuner Γ_T value, 1000 samples are acquired from the VNA. The calibrated data is then used to calculate the standard deviation and shown with red markers in Fig 5(b,c). The same experiment is also conducted with passive stub tuners, and corresponding results are shown with blue markers in Fig 5(b,c).

Then, we propagate the characterized noise $\sigma^2_{|IQ|}$ onto the generated reflection coefficient Γ_T using (7). For this, the input covariance of (6) is determined by assuming $\sigma^2_{|I|}$ and $\sigma^2_{|Q|}$ noise of 2.1 μV for v_I and v_Q baseband signals. The calculated additive noise $\sigma^2_{a,m}$ is then used in (1) and (2) to predict the Γ_T noise, shown in Fig. 5 with dotted lines. Furthermore, the multiplicate noise is estimated using highly mismatched reflection coefficient measurements [8].

Figure 5 shows calculated noise results with lines depicted in red and blue colours for active and passive tuners, respectively. The comparison between the measurement and calculated noise results demonstrates an excellent agreement for magnitude and phase components. The additive noise behaviour predicted with the proposed method strongly agrees with measurement results for low-reflection Γ_T values, as shown in Fig 5b. Furthermore, the noise model results for the active tuner also show an outstanding agreement with the measurement values. These results validate the proposed method for propagating the additive noise using DC v_I and v_Q noise measurements. Furthermore, the active tuner phase noise

measurements also agree with the predicted noise behaviour with (2), shown in Fig. 5(c).
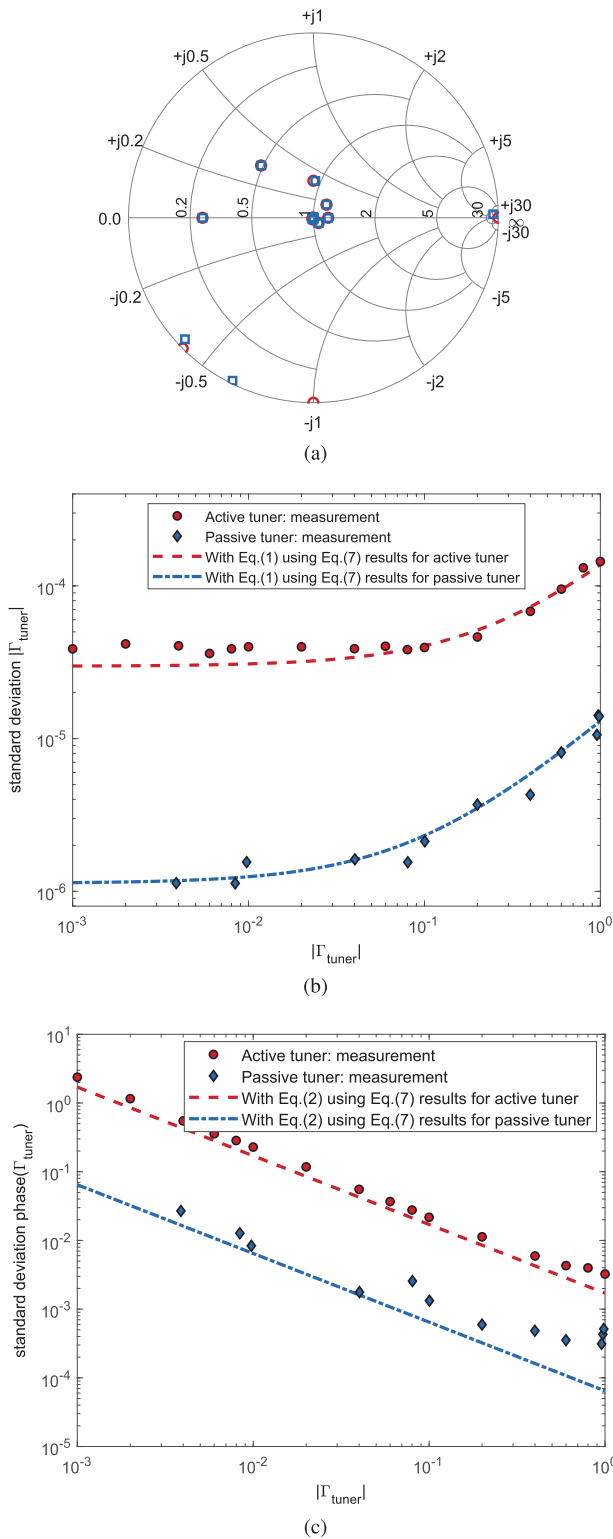

(a)

(b)

(c)

Fig. 5. Noise measurement results for active and passive impedance tuners. (a) Shows the measured impedance values in a 50 Ω normalised Smith chart. (b) Shows noise results for reflection coefficient magnitude. (c) Shows noise behaviour for the reflection coefficient phase.

V. Conclusion

Active impedance tuners employing IQ mixers introduce measurement noise into large-signal measurements. A behavioural model for impedance tuners is proposed to allow the propagation of DC noise from the DACs sourcing the IQ mixer. The additive noise predicted with the proposed method demonstrates an exceptional agreement with the measurement results. Furthermore, a detailed validation of the noise behaviour across the entire Γ_T dynamic of the tuner method is demonstrated with an outstanding agreement. As additive noise affects the magnitude and phase noise behaviour, it is essential to use DAC with low noise behaviour.

References

[1] Y. Takayama, "A New Load-Pull Characterization Method for Microwave Power Transistors," in *MTT-S International Microwave Symposium Digest*. MTT005, pp. 218–220.

[2] V. Teppati, A. Farrero, and M. Sayed, *Modern RF and Microwave Measurement Techniques*. Cambridge University Press, 2013.

[3] M. Marchetti, G. Avolio, M. Squillante, A. K. Doggalli, and B. Anteverta-Mw, "Wideband Load Pull Measurement Techniques: Architecture, Accuracy, and Applications," in *2019 92nd ARFTG Microwave Measurement Conference (ARFTG)*. IEEE, 1 2019, pp. 1–7.

[4] M. Squillante, M. Marchetti, M. Spirito, and L. C. N. de Vreede, "A mixed-signal approach for high-speed fully controlled multidimensional load-pull parameters sweep," in *2009 73rd ARFTG Microwave Measurement Conference*. IEEE, 6 2009, pp. 1–5.

[5] C. De Martino, L. Galatro, R. Romano, G. Parisi, and M. Spirito, "Hardware and Software Solutions for Active Frequency Scalable (Sub)mm-Wave Load–Pull," *IEEE Transactions on Microwave Theory and Techniques*, vol. 68, no. 9, pp. 3769–3775, 9 2020.

[6] K. Lukasik, J. Cheron, G. Avolio, A. Lewandowski, D. F. Williams, W. Wiatr, and D. M. M.-P. Schreurs, "Uncertainty in Large-Signal Measurements Under Variable Load Conditions," *IEEE Transactions on Microwave Theory and Techniques*, vol. 68, no. 8, pp. 3532–3546, 8 2020.

[7] M. Marchetti, G. Avolio, M. Squillante, and A. K. Doggalli, "Load pull measurement techniques: architecture, accuracy, and applications," in *2019 IEEE BiCMOS and Compound semiconductor Integrated Circuits and Technology Symposium (BCICTS)*. IEEE, 11 2019, pp. 1–6.

[8] European Association of National Metrology Institutes, "Guidelines on the Evaluation of Vector Network Analyzers (VNA) - version 3.0," Tech. Rep., 2018.

[9] A. Ferrero, V. Teppati, and A. Carullo, "Accuracy evaluation of on-wafer load-pull measurements," *IEEE Transactions on Microwave Theory and Techniques*, vol. 49, no. 1, pp. 39–43, 2001.

[10] S. Bonino, V. Teppati, and A. Ferrero, "Further Improvements in Real-Time Load-Pull Measurement Accuracy," *IEEE Microwave and Wireless Components Letters*, vol. 20, no. 2, pp. 121–123, 2 2010.

[11] G. Avolio, A. Raffo, J. Jargon, P. D. Hale, D. M. M.-P. Schreurs, and D. F. Williams, "Evaluation of Uncertainty in Temporal Waveforms of Microwave Transistors," *IEEE Transactions on Microwave Theory and Techniques*, vol. 63, no. 7, pp. 2353–2363, 7 2015.

[12] F. A. Mubarak, R. Romano, L. Galatro, V. Mascolo, G. Rietveld, M. Spirito, F. A. Mubarak, and others, "Noise Behavior and Implementation of Interferometer-Based Broadband VNA," *IEEE Trans. Microw. Theory Techn.*, vol. 67, no. 1, pp. 249–260, 1 2019.